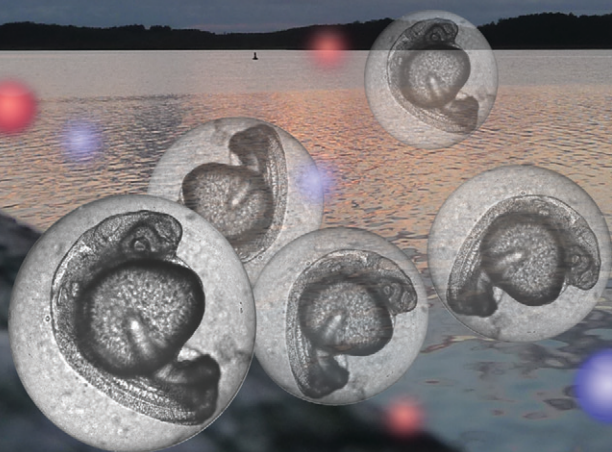
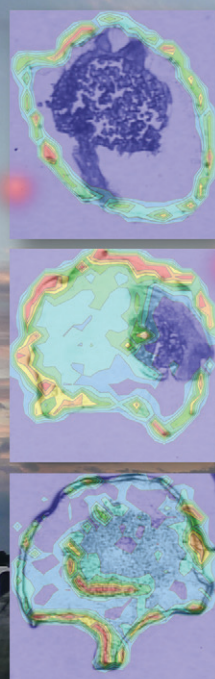


Environmental Science Nano

rsc.li/es-nano



Themed issue: Nanotoxicology in the Environment

ISSN 2051-8153



PAPER

Dana Kühnel *et al.*
Effect propagation after silver nanoparticle exposure in zebrafish (*Danio rerio*) embryos: a correlation to internal concentration and distribution patterns



Cite this: *Environ. Sci.: Nano*, 2015, 2, 603

Effect propagation after silver nanoparticle exposure in zebrafish (*Danio rerio*) embryos: a correlation to internal concentration and distribution patterns†

Steffi Böhme,^a Hans-Joachim Stärk,^b Thorsten Reemtsma^b and Dana Kühnel^{*a}

The zebrafish (*Danio rerio*) embryo (ZFE) is an established ecotoxicological test organism used to investigate the hazardous potential of chemicals. It has been frequently used to test nanoparticles (NPs) for adverse effects. Beyond the assessment of the effects, information on real exposure concentrations, particle uptake and distribution patterns as well as the determination of internal effect concentrations contributes to a deeper understanding of NP–organism interactions. The AgNP and AgNO₃ dose–response curves recorded for different ZFE developmental stages were corrected to real exposure concentrations measured by ICP–MS within this study. Effective concentrations of silver exerting toxic effects were determined by this approach. Organisms showing no effects and individuals with sublethal or lethal effects were compared with regard to silver distribution patterns and internal uptake concentrations in order to allow a more exact correlation. As a result, the internal silver dose per organism differs around 0.5–1 ng Ag per organism irrespective of the developmental stage. However, for earlier developmental stages (2 hours post fertilisation) the ZFE chorion was found to effectively adsorb silver, leading to an up to 20-fold increase in total silver concentrations compared to the later chorion-free stages of the ZFE. Finally, a correlation between increased internal silver (particulate and ionic) concentrations and the occurrence of sublethal and lethal effects was observed.

Received 31st May 2015,
Accepted 5th September 2015

DOI: 10.1039/c5en00118h

rsc.li/es-nano

Nano impact

The zebrafish (*Danio rerio*) embryo (ZFE) is an established *in vitro* test model and can be adjusted towards the toxicity testing of nanoparticles (NPs). However, the chorion represents an effective barrier for particles and therefore, toxic effects may be underestimated. Accordingly, the correlation between the observed adverse effects and internal concentrations was investigated in ZFEs exposed to AgNPs and AgNO₃. Internal silver concentrations were determined and combined with the toxicological information to obtain critical internal effect concentrations triggering biological responses. Furthermore, toxicological points of action were visualised and morphological changes during the occurrence of toxic effects were observed.

Introduction

In general, the observation of biological effects at certain concentrations is used to calculate dose–response curves, delivering effect concentrations (*e.g.*, EC₅₀-values) and thus allowing the estimation of the toxic potential of a substance. However, by applying nominal concentrations for the calculation of effect concentrations, toxicity is underestimated in case of a

substance loss from exposure solutions. Indeed, for some nanoparticles (NPs), the real exposure concentrations are reported to be lower compared to the amounts of nominal exposure.^{1,2} As a consequence, the analytical measurement of exposure concentrations, especially for NPs, is necessary to correctly determine the toxicity of a substance and to perform an appropriate risk assessment.³

The zebrafish (*Danio rerio*) embryo (ZFE) toxicity test is a versatile *in vitro* model used to assess the hazardous potential of chemicals. It has been applied in several studies for the toxicological testing of NPs.^{4–6} The ZFE, as a vertebrate model species, combines advantages such as rapid development, easy maintenance in the laboratory, a large number of offspring, transparency of embryos and access to experimental manipulation to avoid expensive animal

^a Helmholtz Centre for Environmental Research - UFZ, Department of Bioanalytical Ecotoxicology, Permoserstrasse 15, 04318 Leipzig, Germany. E-mail: dana.kuehnel@ufz.de

^b Helmholtz Centre for Environmental Research - UFZ, Department of Analytical Chemistry, Permoserstrasse 15, 04318 Leipzig, Germany

† Electronic supplementary information (ESI) available: Additional information is available. Fig. S1: Dose–response curves of AgNPs and AgNO₃ after 48 h exposure. See DOI: 10.1039/c5en00118h



testing.⁷ It allows the observation of acute lethal and sub-lethal (*e.g.*, oedema, pigmentation, hatching) toxicological endpoints.

In addition, the ZFE test allows complementing the effect-based toxicity data with internal concentrations obtained by accumulation studies. The correlation between potential toxicological effects and internalised concentrations was already performed for ZFEs exposed to different organic chemicals.^{8,9} However, data for the accumulation of NPs in the ZFE are required with regard to the quantification of internal concentrations and the visualisation of the particle distribution. Suitable analytical methods are needed which cover the requirements of high (elemental) sensitivity and spatial resolution to detect NPs within biological tissues.¹⁰ Mainly electron microscopy (SEM, TEM),¹¹ fluorescence microscopy,^{12,13} and inductively coupled plasma mass spectrometry (ICP-MS)^{5,6} were applied in recent studies.

NP accumulation at or within the ZFE chorion structures has been observed, assuming a particle barrier function of the chorion.^{12,13} The yolk syncytial layer was described as the target structure for AgNPs, indicating that the particle interaction with this structure is inducing toxicity.¹ Furthermore, the embryo surface is suggested as an accumulation site potentially leading to an uptake of particles or ions *via* the skin. However, there is no evidence of NP or ion incorporation within the embryo tissues.^{1,13} As a consequence, it is not fully clear how the interaction of NPs with the whole embryo leads to the propagation of toxic effects.

In order to improve the analytical detection of NPs associated with environmental organisms, we optimised ICP-MS-based techniques in order to determine the internal concentrations and gain information on the elemental distribution within the organism. Therefore, neb-ICP-MS was adopted for the quantification of metal-based NPs. Laser Ablation ICP-MS (LA-ICP-MS), a 2D imaging technique, was developed to visualise the NP distribution within organisms.^{14,15}

Different developmental stages of ZFEs (*e.g.* to be concise, stages with and without chorion) were exposed to AgNPs to address the gap between the information based on observed toxicological effects and quantitative internal NP concentrations. Subsequently, (1) dose-response curves obtained for the different stages were corrected for real exposure concentrations, (2) internal concentrations were determined, and (3) the distribution of silver in embryos which showed no damage, sublethal or lethal effects were compared. Furthermore, recent studies reported a high impact on toxicity by the dissolved silver ion fraction, released from the particle surface.^{16,17} Hence, in addition to AgNPs, AgNO₃ exposures were included in the study to demonstrate whether substantial differences in AgNP and silver ion uptake and distribution exist. The aim of this study was to identify toxicological points of action and gain information on the propagation of toxic effects related to an AgNP exposure.

Materials and methods

Zebrafish cultivation and selection

Zebrafish (*Danio rerio*) embryos were exposed to AgNPs and AgNO₃ according to the OECD test guideline 236.¹⁸ The organisms were cultured at 26 ± 1 °C at a 14:10 h light:dark cycle. The fishes were fed with *Artemia spec.* on a daily basis. For the egg collection, spawn traps covered with a wire mesh were placed into fish tanks on the day prior to spawning. After the selection, the fertilised eggs were transferred to ISO-water (294.0 mg l⁻¹ CaCl₂·2H₂O, 123.3 mg l⁻¹ MgSO₄·7H₂O, 63.0 mg l⁻¹ NaHCO₃, and 5.5 mg l⁻¹ KCl dissolved in deionised water) and different developmental stages of the ZFEs were used for the toxicity and accumulation studies (Table 1). The 26 hours post fertilisation (hpf) ZFEs were dechorionated prior to testing by a mechanical dechoriation with forceps. All experiments involving zebrafish embryos were performed in compliance with the relevant laws and institutional guidelines, and the institution has all relevant permissions to breed zebrafish.

Nanoparticle characterisation

The AgNPs used in this study were provided and characterised in detail by the partners of the EU project NanoValid (www.nanovalid.eu, internal draft).¹⁹ The main characteristics were summarised in Table 2. Briefly, the AgNPs were characterised by a primary particle size of 10–21 nm, a hydrodynamic particle size of 117 ± 24 nm, and a polyvinyl pyrrolidone (PVP) coating. The primary particle sizes were assessed by electron microscopy techniques (SEM, TEM) and nanoparticle tracking analysis (NTA). Furthermore, dynamic light scattering (DLS) was applied to determine the particle size distribution and the zeta potential of the AgNPs in the stock suspension.

AgNO₃ (ICP-MS standard, 1 g l⁻¹, Merck) was used as positive control to assess the influence of ionic silver on toxicity and uptake. The silver exposure solutions for toxicity and accumulation studies were prepared in ISO-water just before the start of testing. The dissolved silver ion fraction was determined for the stock suspension as well as for the different concentrations of the exposure suspensions in ISO-water (for AgNPs). Therefore, the samples were centrifuged for 30 min at 16 000 g. After centrifugation, the amount of dissolved silver in the supernatant was measured by ICP-MS and the residue was digested and analysed for the total silver concentration.

Exposure of ZFE for effect assessment

The AgNP and AgNO₃ exposure solutions in a concentration range of 0–1000 µg l⁻¹ were freshly prepared by dilution in ISO-water prior to testing. The exposure experiment was conducted in 24-well plates with one individual and 2 ml exposure media per well. In total, 10 individuals per concentration were used and a minimum of 3 replicates was performed. Samples of the exposure solutions were taken



Table 1 Developmental stages (stadium) of the ZFE chosen for experiments; the age at the onset of exposure is given




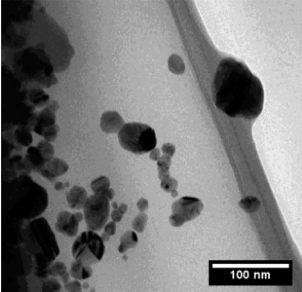
	Stadium	Description	Characteristics
	2 hpf	Whole organism	Organism including embryo and chorion
	26 hpf	Dechorionated embryo	Mechanical dechorionation at 24 hpf, no chorion
	71 hpf	Hatched embryo	Naturally hatched embryos, no chorion

Table 2 Chemical and physical properties of AgNP stock suspension and exposure suspensions¹⁹

	Parameters	Stock suspension	Exposure suspension (100 $\mu\text{g l}^{-1}$)
	Shape	Spheres	Spheres
	X_{TEM}	21 ± 8 nm	—
	X_{AFM}	13 ± 9 nm	—
	X_{NTA}	10–150 nm	—
	Coating	PVP	PVP
	X_{DLS}	117 ± 24 nm	135 nm
	Zeta potential	-19 ± 9 mV	—
	Dissolved fraction	$48.3 \pm 7.2\%$	$44.3 \pm 5.3\%$

prior to testing in order to analyse the silver concentrations by ICP-MS measurements. The toxicological effects were assessed after exposure periods of 24 h and 48 h according to the OECD guideline 236.¹⁸ In this context, sublethal effects are defined as edema (yolk, pericard), change of pigmentation or heart frequency, a missing blastula, epiboly, or adverse eye formation. Coagulation, missing formation of somites, no detachment of tail and no heartbeat are indicators for lethality. The dose-response curves representing the percentage of lethality against the exposure concentrations and the EC_{50} -values were calculated using GraphPad Prism 5.

Exposure of ZFE for accumulation studies

Nominal AgNP and AgNO_3 concentrations up to $150 \mu\text{g l}^{-1}$ were used for the exposure in the accumulation studies. Exposure concentrations of $100 \mu\text{g l}^{-1}$ AgNPs or AgNO_3 were applied for the determination of the silver distribution in the ZFE of different developmental stages by LA-ICP-MS. Five individuals were exposed in glass petri dishes with a total exposure media volume of 10 ml. In parallel, samples of the exposure solutions were taken prior to exposure in order to analyse the concentrations by ICP-MS. The Ag speciation was calculated for both AgNP and AgNO_3 exposures by using Visual MINTEQ (Visual MINTEQ, ver. 3.1, 2013, KTH, Sweden).²⁰ The calculation was based on the measured dissolved Ag in the respective exposure suspension. The pH was set to 7.6 and temperature to 26 °C.

For the subsequent correlation of observed effects to the internal concentrations, ZFE showing either no toxic effects, sublethal, or lethal effects were selected and collected for the elemental analysis. In order to obtain a sufficient amount of sample material, three individuals per concentration were pooled for one sample. The organisms were washed twice with the medium after 24 h exposure, shock frozen and digested for the neb-ICP-MS measurements. The washed organisms were fixated with a paraformaldehyde phosphate buffered solution, embedded with frozen section medium (Neg-50, Richard Allen Scientific) and cut in $40 \mu\text{m}$ sections by a microtome (MICROM Cryo Star, HM560, Thermo Scientific) at -20 °C. The sections were placed on glass slides and were introduced to the laser ablation system for the imaging by LA-ICP-MS.

ICP-MS measurements

A quadrupole-based ICP-MS (ELAN DRCe, Perkin Elmer Sclex) was applied to quantify the silver concentrations within the exposed organisms. The AgNP- or AgNO_3 -exposed ZFEs were digested with 30% nitric acid (65%, suprapur, Merck) in an open digestion system (DigiPrep, S-Prep). The homogeneous samples obtained after digestion were analysed for their silver concentrations by neb-ICP-MS. An external calibration was performed by analysing an AgNO_3 standard reference solution (1 g l^{-1} , Merck).



The sections were ablated by a Nd:YAG laser (LSX 500, CETAC, USA) with a wavelength of 266 nm for the visualisation of the silver distributions within the embryos by LA-ICP-MS. The laser energy was adjusted to 60% to ensure a complete ablation of the organic layer. The generated particle aerosol was directly transported and introduced to the ICP-MS via an additional argon gas stream. A 50 μm spot diameter for the spot ablation was chosen to avoid measurement times above 4 h for one organism section. An external calibration was performed by applying individual particle-spiked agarose gels in accordance with an earlier protocol.¹⁵ The transient intensity signals for the individual spots were collected in a data matrix and converted to concentrations using the calibration curves. Both the exact parameters for the transformation into a 2D-color plot and the LOD of the applied semi-quantitative LA-ICP-MS technique (35.7 fg Ag/50 μm spot) were reported earlier.¹⁴

Results and discussion

In order to gain insight into the propagation of toxic effects exerted by NPs in ZFEs, systematic exposure experiments of the developmental stages (Table 2) with and without chorion, and a range of AgNP and AgNO₃ concentrations were performed. As knowledge on external and internal silver concentrations is vital, classical concentration response testing was complemented by analytical determination of silver concentrations and distribution in the experimental system.

External exposure conditions

The silver concentrations determined in the prepared exposure solutions differ significantly from the nominal ones with a recovery of $63 \pm 12\%$ and $55 \pm 11\%$ for AgNO₃ and AgNPs, respectively. This is in line with previous studies on AgNPs, describing similar differences between nominal and measured concentrations.^{1,2} The loss of silver from the exposure system may be accounted to the adsorption to the surroundings such as the walls of the exposure vessels, pipette tips, or the agglomeration and sedimentation of particles.³ The precipitation of silver as AgCl and a subsequent concentration loss is another phenomenon described in the literature.²¹ As a consequence, the bioavailable silver fraction is reduced which might reduce the efficiency of the digestion and subsequent ICP-MS analysis. As indicated by the saturation index calculated for the Ag species distribution within the exposure suspensions, no precipitation of AgCl(s) can be expected.

The OECD guidance document on the handling of difficult substances recommends that the difference between nominal and real concentrations should not exceed $\pm 20\%$,²² otherwise corrective actions concerning exposure design or calculation of results are needed. Whether this recommendation is also applicable to NPs is currently under debate.²³ Usually, effect concentrations are expressed as nominal concentrations which can result in high variabilities between studies³ as reported by Escher and Hermens.²¹ Toxicity and quantitative

data were corrected to measured concentrations as a consequence.

In addition, a large dissolved silver ion fraction (44–48%) was detected within the AgNP stock and exposure suspensions, which is constant over time. This is in agreement with the literature data on silver dissolution in PVP-coated AgNP suspensions showing that up to 40% of the silver is present in the ionic form.¹⁷ Hence, only small differences in the toxicity of AgNPs and AgNO₃ are to be expected, as the dissolved silver dominates in both exposures. The comparability of both exposures was demonstrated by the calculation of the identical shares of the different silver species for both exposures, with 66% AgCl(aq), 23% AgCl²⁻, and 10% dissolved Ag⁺. The observed effects and measured uptake concentrations were directly compared as a consequence.

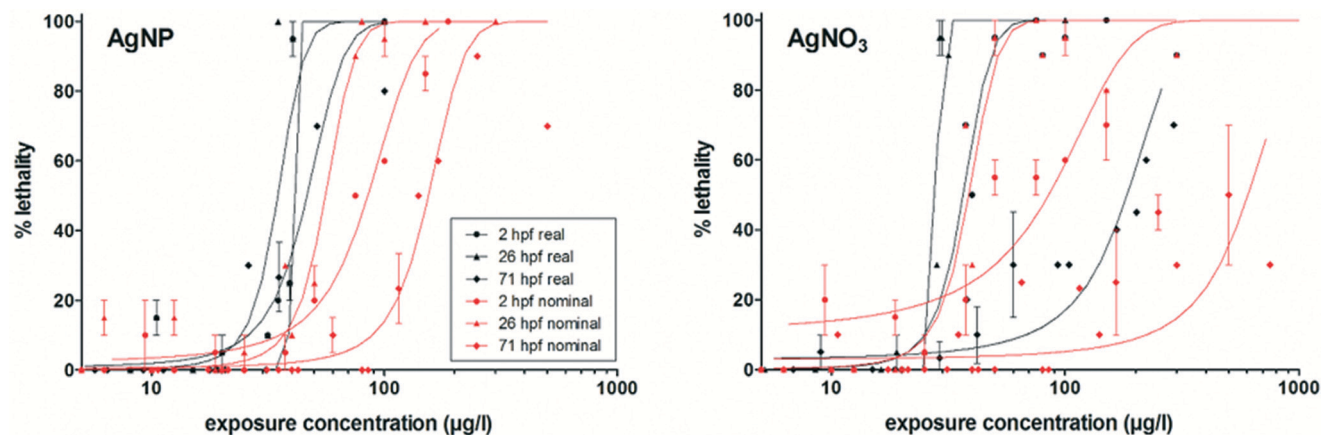
Toxicity assessment and correction to real exposure concentrations

The following steps were performed for a complete toxicity assessment: (1) ZFE toxicity testing of AgNPs and AgNO₃ according to the OECD test guideline 236, (2) correction of calculated dose–response curves and the LC₅₀-values using measured, real silver concentrations, and (3) comparison of the obtained results based on nominal and corrected exposure concentrations. The corrected effect concentrations compared to the nominal effect concentrations were shown in Fig. 1. A concentration-dependent toxicity was observed for AgNP and AgNO₃ treated ZFEs.

The most sensitive developmental ZFE stage was 26 hpf, followed by 2 hpf and 71 hpf, for both AgNPs and AgNO₃ exposures based on nominal concentrations. On the contrary, the LC₅₀-values corrected for the measured silver concentrations were comparable with the different ZFE developmental stages (Fig. 1). One exception was the corrected LC₅₀-value of the AgNO₃ of ZFEs exposed at 71 hpf, indicating a lower sensitivity of the later developmental stage towards ionic silver. However, the corrected LC₅₀-values of AgNPs and AgNO₃ were in the same concentration range of 30–40 $\mu\text{g l}^{-1}$ (corresponding to 0.28–0.38 μM), indicating that the toxicity is independent of the ZFE stadium upon the start of the exposure experiment. After 48 h exposure, the LC₅₀-values were comparable to the 24 h effect values as reported in the ESI,† Fig. S1. Based on the amount of dissolved silver (Fig. 1), the differences in LC₅₀-values of 71 hpf ZFEs were confirmed. In this case, the higher toxicity of AgNPs can be related to an enhanced dissolution of particles at the contact site of the organism after an increased exposure to AgNPs of this ZFE stadium due to the higher mobility of the organisms.

Groh *et al.*²¹ described toxicity to be dependent on the developmental stage of the ZFE, with a higher sensitivity during the earlier stages. On the contrary, Asharani *et al.*¹¹ reported ZFEs in the 4–6 hpf stages as more resistant. However, both studies applied nominal concentrations for their dose–response modelling and the calculation of LC₅₀-values. The results of our study showed that the presence or absence





Exposure start	AgNP LC ₅₀ (µg/l)			AgNO ₃ LC ₅₀ (µg/l)		
	nominal	real	based on Ag ⁺	nominal	real	based on Ag ⁺
2 hpf	80.4 ± 7.8	39.5 ± 0.5	1.7	70.5 ± 20.8	36.1 ± 2.6	3.6
26 hpf	55.0 ± 6.0	34.4 ± 6.6	1.5	38.1 ± 4.3	28.5 ± 0.1	2.9
71 hpf	150.0 ± 13.4	45.1 ± 5.0	2.0	795.8 ± 345.1	185.9 ± 24.3	18.6

Fig. 1 Dose-response curves based on nominal (red) and corrected real exposure concentrations (black) for the respective developmental stages of the ZFE. The calculated nominal and real LC₅₀-values of the respective AgNP or AgNO₃ exposure as well as the developmental stage are listed in the table below. The LC₅₀-values based on the dissolved Ag⁺ were calculated according to the ionic silver content in the exposure solution.

of the chorion around the embryo did not significantly influence the toxic potency of the silver. That is in agreement with Cunningham *et al.*¹⁷ observing similar toxicological results for both ZFE with and without chorion.

Groh *et al.*²¹ collected and reported LC₅₀-values for silver-exposed ZFEs ranging from 0.1 nM–820 µM for AgNPs and around 0.75 µM for AgNO₃. The LC₅₀-values obtained in this study are well within this range. With regard to the reported LC₅₀-value of AgNO₃, our results for AgNPs and AgNO₃ (LC₅₀ ~0.33 µM) corrected for real concentrations match quite well. The LC₅₀-values for AgNPs and AgNO₃ were comparable. Hence, the toxicity may be attributed to dissolved silver alone, as both the AgNPs and AgNO₃ exposure contained the same share of dissolved silver. A major impact of the bio-available ionic fraction on the acute toxicity of AgNPs towards zebrafish embryos was reported by previous studies.^{1,20,24} Furthermore, the study of Bar-Ilan *et al.*²⁵ stated that the sequence and type of events leading to the death of zebrafish embryos are similar for AgNPs and ionic silver. In contrast, Yue *et al.*²⁶ demonstrated a particle-specific effect on RTgill-W1 cells with higher toxicity of cit-AgNP in comparison to AgNO₃ exposures if related to the dissolved silver fraction.

Quantification and visualisation of silver accumulation in ZFEs in the absence of toxicological effects

The ZFEs of different developmental stages were exposed to concentrations up to 150 µg l⁻¹ for 24 h. Only living and intact organisms were selected to be analysed by ICP-MS in order to obtain the internal concentrations. In addition, ZFEs

exposed to 100 µg l⁻¹ were sectioned and the elemental distribution was visualised by LA-ICP-MS.

The ZFEs exposed at 2 hpf are characterised by the chorion structure surrounding the embryo.²⁷ Silver concentrations of 15 ng Ag per organism for AgNPs and 8 ng Ag per organism for AgNO₃ were measured for 2 hpf ZFEs after 24 h exposure (Fig. 2). Furthermore, a clear concentration-dependent increase in internal silver concentrations was observed for ZFEs exposed to AgNO₃ at 2 hpf whereby a higher variability between the exposure concentrations and the internal concentrations was observed for AgNPs. The differences between the measured silver concentrations of AgNP- and AgNO₃-exposed ZFEs may be attributed to the presence of the chorion. The adsorption and binding processes of the particulate and ionic silver to the chorion's structure were expected to be different and may lead to the observed differences in the silver concentrations for ZFEs exposed at 2 hpf. Auffan *et al.*²⁸ observed a complex formation between citrate-capped Ag-NPs and thiolated sites of proteins and enzymes of the chorion of Atlantic killifish embryos.

ZFEs without chorion (26, 71 hpf) showed lower silver concentrations for both AgNP and AgNO₃ exposures compared to the ZFEs exposed at 2 hpf. In detail, concentration means of 0.2 and 0.7 ng Ag per organism were measured for 26 hpf and 71 hpf ZFEs treated with AgNPs, respectively (Fig. 2). The internal uptake concentration for chorion-free development stages was independent of the exposure concentration.

These findings indicated that the ZFE chorion played a crucial role in the adsorption of silver irrespective of the type



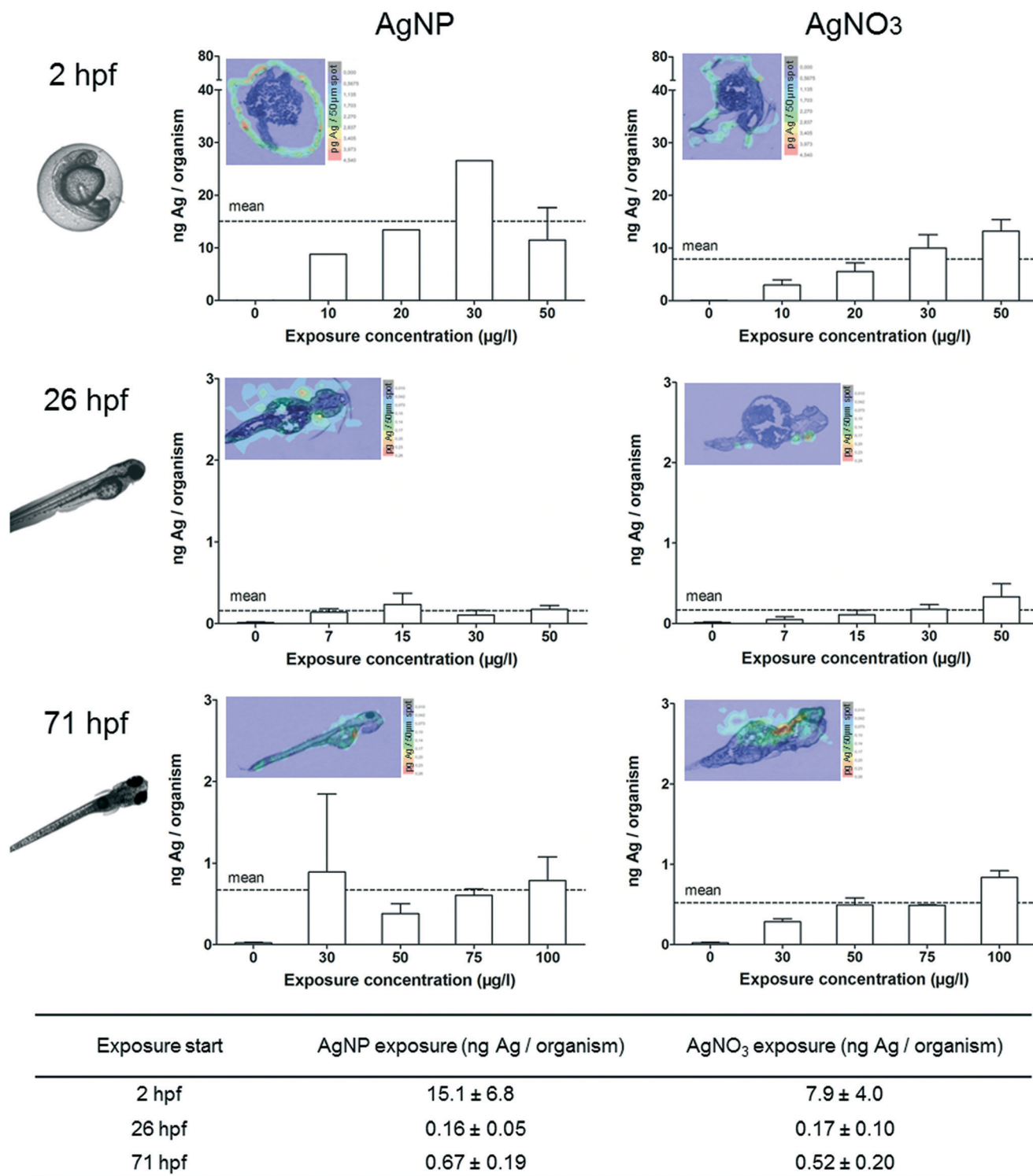


Fig. 2 Silver concentrations measured for ZFE exposed at different developmental stages (2, 26, and 71 hpf) in the absence of toxicological effects. Quantification results obtained by neb-ICP-MS and respective LA-ICP-MS images after 24 h of exposure are shown. The color scale bar of the LA-ICP-MS measurements represents silver concentrations from the highest (red) to the lowest value (blue). The table below shows the calculated means over the exposure concentrations (dotted lines in graphs).

(particular or ionic), resulting in up to 20-fold higher silver concentrations in the organisms compared to the chorion-free stages. By the visualisation *via* LA-ICP-MS, the

accumulation of silver at or within the chorion structures for ZFEs of the 2 hpf developmental stage became obvious (Fig. 2).



The association of AgNPs or Ag-nanoplates to the chorion structure without a direct uptake of particles by the embryo was previously observed by George *et al.*²⁹ and Osborne *et al.*¹ In contrast, Asharani *et al.*¹¹ and Lee *et al.*³⁰ detected

an incorporation of single AgNPs within the perivitelline space (PVS) located between the chorion and the embryo or even within the embryonic tissues. These contrasting findings may be caused by the influence of the particle properties

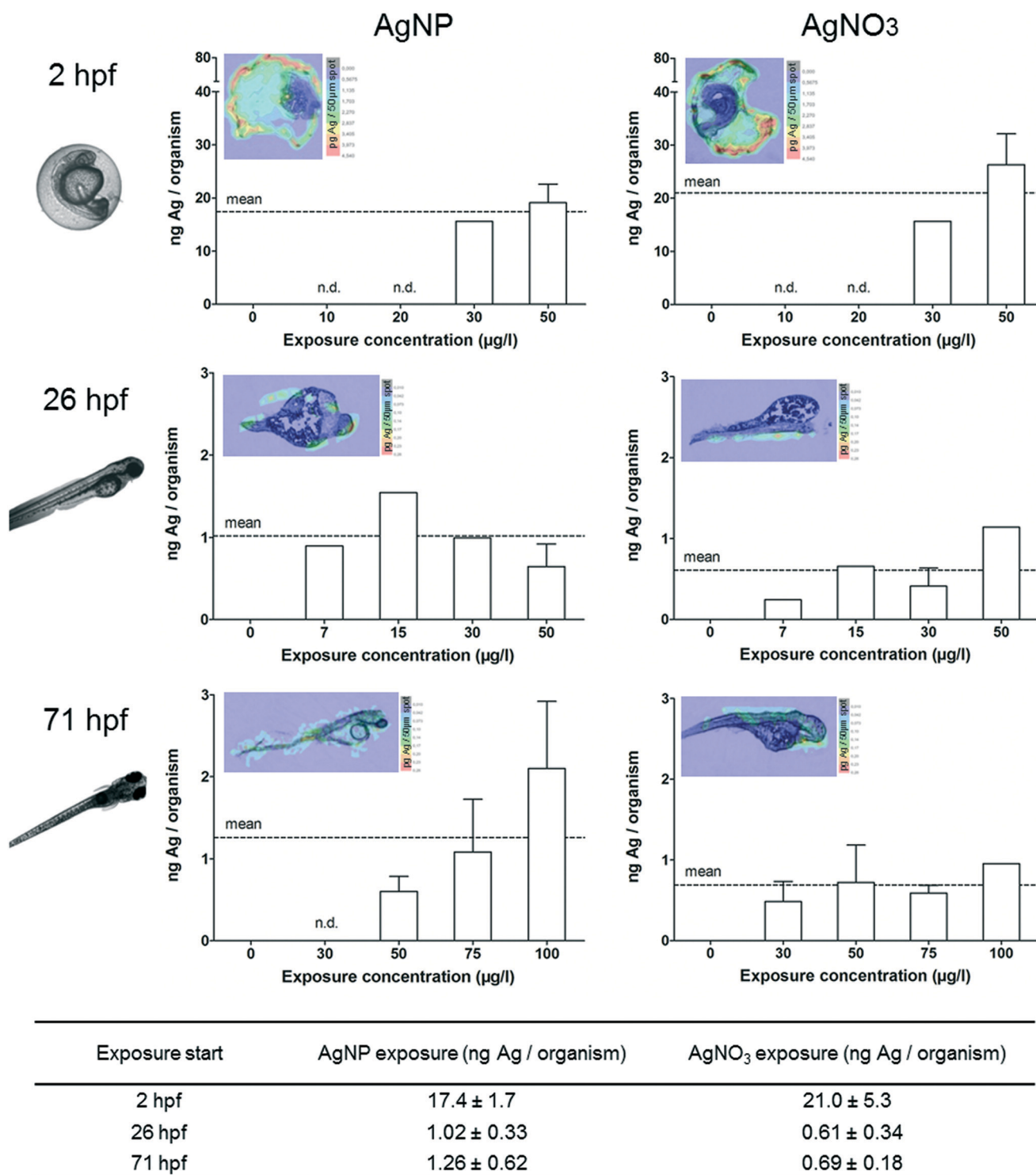


Fig. 3 Silver concentrations measured for ZFE exposed at different developmental stages (2, 26, and 71 hpf) in the presence of sublethal effects. Quantification results obtained by neb-ICP-MS and respective LA-ICP-MS images after 24 h of exposure are shown. The color scale bar of the LA-ICP-MS measurements represents silver concentrations from the highest (red) to the lowest value (blue). The table below shows the calculated means over the exposure concentrations (dotted line in graphs).



such as the coating and size of the particles³¹ and the exposure duration on the internalisation process. For example, Asharani *et al.*¹¹ applied small and stabilised AgNPs (5–20 nm) which were able to pass through the chorion pore channels and reach the embryo. The transport of 12 nm AgNPs through the chorion pore channels into the inter ZFE compartments was examined after short exposure durations of 0–2 h in the study of Lee *et al.*³⁰

The above mentioned studies determined either (1) the real NP concentrations in exposure suspensions, (2) the measured quantitative AgNP uptake concentrations or (3) they visualised the silver distribution within the organisms. However, a combination of the three parameters is needed. Furthermore, the influence of the developmental stage of the ZFE on the uptake and distribution of silver was not examined so far. Two studies reported quantification results for ZFEs with intact chorion. The study of George *et al.*²⁹ on Ag-nanoplates reported silver concentrations of 400–450 ppb per ZFE for 4 hpf ZFE treated with 5 mg l⁻¹ for 48 h corresponding to an uptake of 0.3–0.4 ng per ZFE, assuming an organism volume of 800 nl. In addition, Auffan *et al.*²⁸ measured a total AgNP concentration of 60–140 ng per organism for Atlantic killifish (*Fundulus heteroclitus*) embryos exposed to 5 mg l⁻¹ and 48 h.

Silver particle and ion distribution patterns for ZFEs showing sublethal effects

In order to investigate the silver accumulation during the occurrence of toxicological effects, individual ZFEs showing sublethal effects such as edema (yolk, pericard), change of pigmentation or heart frequency were selected and collected. Especially the occurrence of edema was prominent during the exposure with AgNPs and AgNO₃. The observed sublethal effects are in accordance with other studies which reported interruptions in the cardiac cycle, edema, or hatching delays.^{11,16} The quantification and visualisation results were presented in Fig. 3. No individuals showing effects could be collected (n.d.-not determined) or solely single individuals were analysed (no error bar) for some exposure concentrations.

All individuals showing sublethal effects accumulated increased silver concentrations compared to ZFEs showing no effects. The following silver concentrations were measured after a 24 h AgNP exposure for ZFEs exposed at 2, 26, and 71 hpf: 17.4, 1.0, and 1.3 ng Ag per organism, respectively. A concentration-dependent uptake was observed for the 2 hpf (both for AgNP and AgNO₃ treatment) and the 71 hpf ZFE stage (only for the exposure with AgNPs). Differences between the uptake concentrations of AgNPs and AgNO₃ were only measured for ZFEs exposed at 71 hpf with higher silver concentrations for organisms exposed to AgNPs. Probably, the enrichment of particles at the embryo surface leads to a subsequent release of silver ions into the embryonic tissues for this later developmental stage. Furthermore, the ZFE of this

developmental stage is more mobile, implying a potentially higher exposure to AgNPs.

The silver distribution for 2 hpf ZFEs showing sublethal effects was different compared to the silver distribution within ZFEs lacking toxicological effects. As visible *via* the LA-ICP-MS imaging, silver was not only detected at the chorion, but also in the perivitelline space (PVS). This compartment is hard to sample individually but the silver accumulation in the PVS can be easily detected by LA-ICP-MS. However, it was not possible to distinguish between silver particles or the silver ion fraction by using this method. Since we detected a high fraction of ionic silver in the AgNP suspensions, the main proportion detected in the PVS might be attributed to dissolved silver ions. The NP-chorion interaction seems to result in a higher permeability of the chorion, and therefore more silver was detected within the PVS. Once silver is accumulated in the PVS, the translocation of silver to the embryo surface is likely. This was indeed observed for the later developmental stages (26, 71 hpf) (Fig. 3).

Concerning the number and sizes of particles, Lee *et al.*³² qualitatively showed that deformed ZFEs internalised larger and a higher number of AgNPs compared to normally developed embryos of 120 hpf. The potential of metal oxide NPs to reach the embryo surface and to penetrate the skin triggering toxic effects was described previously by Lin *et al.*¹³ and Zhu *et al.*³³ In this context, Osborne *et al.*¹ described the yolk syncytial layer as the target tissue for AgNPs resulting in the passage of particles into the yolk, an uptake by the embryo, and subsequently the occurrence of adverse effects or lethality. Furthermore, the release of silver ions from AgNPs accumulated in the ZFE due to a particle destabilisation was theoretically described by Bar-Ilan *et al.*²⁵ and van Aerle *et al.*²⁴

Silver accumulation assessment in lethal ZFEs

In order to determine the silver accumulation in dead embryos, we selected and collected individual ZFEs showing one of the following parameters according to the OECD test guideline 236:¹⁸ coagulation, missing formation of somites, no detachment of tail or no heartbeat. No individuals showing effects could be collected (n.d.-not determined) or solely single individuals were analysed (no error bar) for some exposure concentrations. For all we know, this is the first study quantifying NP uptake within dead ZFEs.

As described for ZFEs with sublethal effects, dead ZFEs also showed higher internal silver concentrations compared to intact, living organisms. In general, no differences between AgNP or AgNO₃ exposure were observed for dead ZFEs. The silver concentrations determined for the chorion-free stages were comparable to those of ZFEs showing sublethal effects, with 0.9 (26 hpf) and 1.2 ng Ag per organism (71 hpf) for a 24 h AgNP exposure. Only for ZFEs exposed at 2 hpf, probably due to the presence of the chorion, a two-fold increase in accumulation compared to ZFEs showing sublethal effects was observed, *e.g.*, 33 ng Ag per organism for AgNP exposed organisms.



However, the denaturation of the ZFEs upon death results in physically defect organisms. This leads to huge standard deviations of the silver concentrations measured for 2 hpf ZFEs, indicating technical constraints when

sampling and analysing silver concentrations of dead ZFEs with chorion.

In addition, the silver distribution in ZFEs changed over time. The highest silver concentrations at 2 hpf are located in

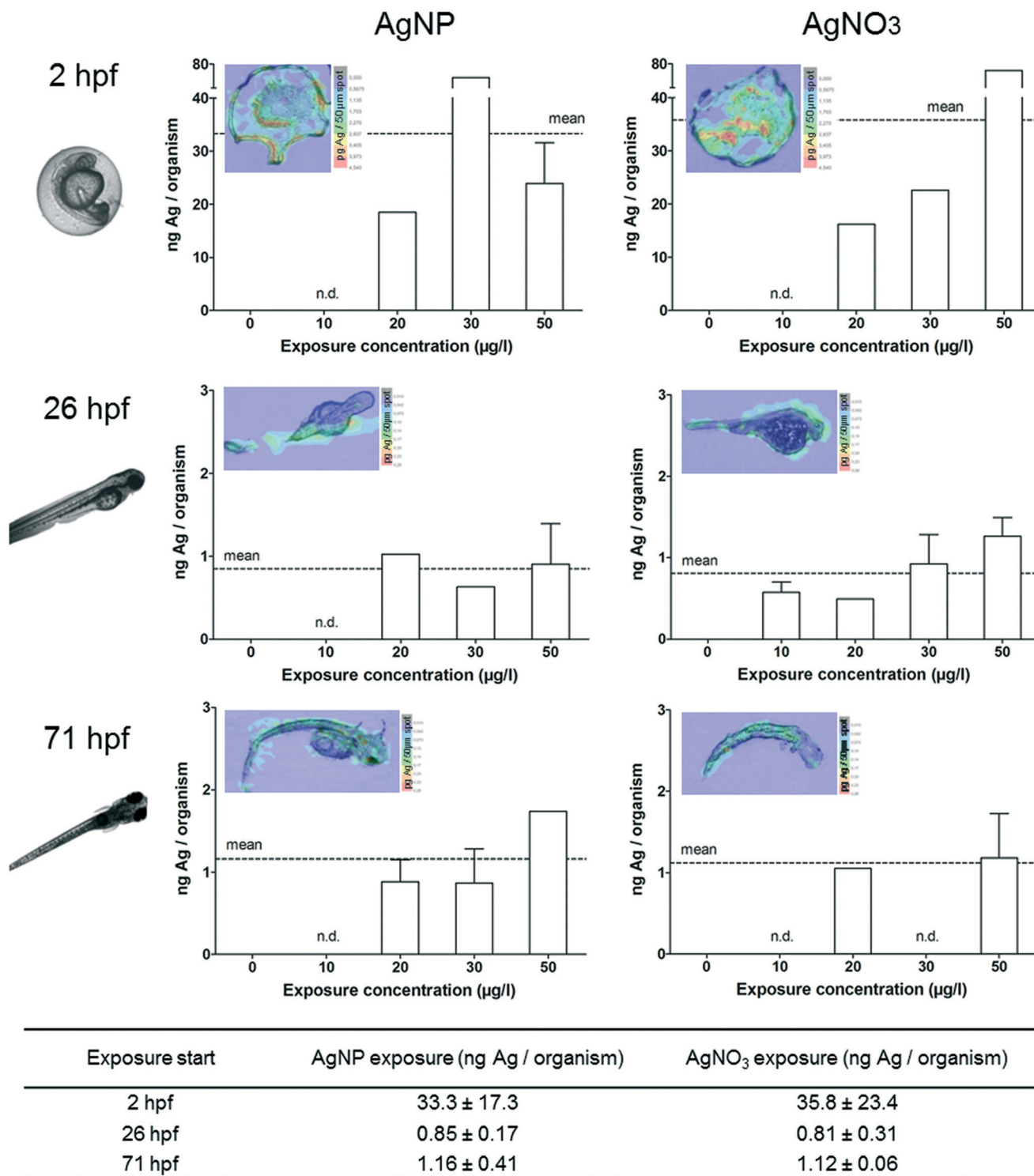


Fig. 4 Silver concentrations measured for dead ZFE exposed at different developmental stages (2, 26, and 71 hpf). Quantification results obtained by neb-ICP-MS and respective LA-ICP-MS images after 24 h of exposure are shown. The color scale bar of the LA-ICP-MS measurements represents silver concentrations from the highest (red) to lowest value (blue). The table below shows the calculated means over the exposure concentrations (dotted line in graphs).



the dead embryo tissue as shown by LA-ICP-MS measurements (Fig. 4). The enrichment in this specific ZFE compartment is similar for both particulate and ionic silver. Silver accumulation at the surface of the embryo (26 hpf) and silver distribution within the embryo tissue (71 hpf) are again observed for the later ZFE stages. However, it remains unclear, whether the increase in internal silver concentrations in damaged embryos is a cause of toxicity or its consequence.

Correlation between toxicological effects and internal concentrations

The toxicological testing of AgNPs and AgNO₃ revealed comparable LC₅₀-values for the different developmental ZFE stages related to the measured exposure concentrations. As a consequence, the presence of the chorion alone seems to have no mitigating effect on silver toxicity.

In contrast, the quantification and visualisation data obtained for AgNP and AgNO₃ exposed ZFEs differ with respect to the developmental stage. The chorion has a tremendous impact on the amount of silver detected based on the measurement of silver associated to the ZFE. Especially, distinct differences in the internal silver concentrations and distribution patterns were detected for the first developmental stage (2 hpf) due to the presence of the chorion. This phenomenon was compared in 26 hpf ZFEs, with and without chorion, but no differences in the internal silver concentrations of the embryos were measured (data not shown). The structure of the chorion adsorbed substantial amounts of silver, which, however, did not influence the toxicity effects. Likewise, the presence of the chorion influenced the silver distribution upon occurrence of sublethal and lethal effects. The internal silver concentrations and distribution patterns were comparable for chorion-free stages (26 hpf, 71 hpf) even for ZFEs showing adverse effects.

The toxicological effects at different developmental stages were correlated with the respective internal concentrations

(Fig. 5). The 2 hpf stage enclosed by the chorion was excluded from the correlation since the chorion was identified as the major adsorption site for AgNPs and would hence disturb the correlation. Thus, we referred to the internal concentration measured for the embryo since the attachment to the outer surface and the direct internalisation of silver in the embryonic tissues were described as the main mechanism leading to toxicity.^{1,11}

The correlation revealed an effect-related increase in internal ZFE concentrations (Fig. 5) as a higher percentage of effect (sublethal or lethal) is linked to a slight increase in the internal silver concentration. In general, the silver concentrations obtained for ZFEs showing adverse effects vary between 0.5–1 ng Ag per organism for both AgNPs and AgNO₃. This further indicates that the results are independent of the silver entity introduced to the organism. However, the progression of the effects over time is still not fully resolved, and it remains unclear, whether the increase in silver uptake is the cause or the result of damage to ZFE tissues.

To our knowledge, this is the first direct correlation of the effect values and internal concentrations based on AgNP exposure. Lee *et al.*³⁰ reported a dependency of toxicity on the exposure concentration with a critical concentration of 0.19 nM AgNPs (~21 ng), which matches our results. However, we extended the observation of toxicity by determining the critical internal dose (0.5–1 ng Ag per organism) directly affecting the embryo. Nevertheless, further measurements are necessary to validate the presented internal effect concentrations.

We assume that sublethal and lethal effects occur upon accumulation of a critical silver dose within the embryo. This is in agreement with Escher and Hermens³ describing this relationship for substances leading to an irreversible biological effect. Furthermore, this is in line with the assumption that NPs behave differently from chemicals, which penetrate the chorion and build an equilibrium of internal and external concentration by simple diffusion. In the case of NPs, the particle uptake is driven by kinetically controlled particle

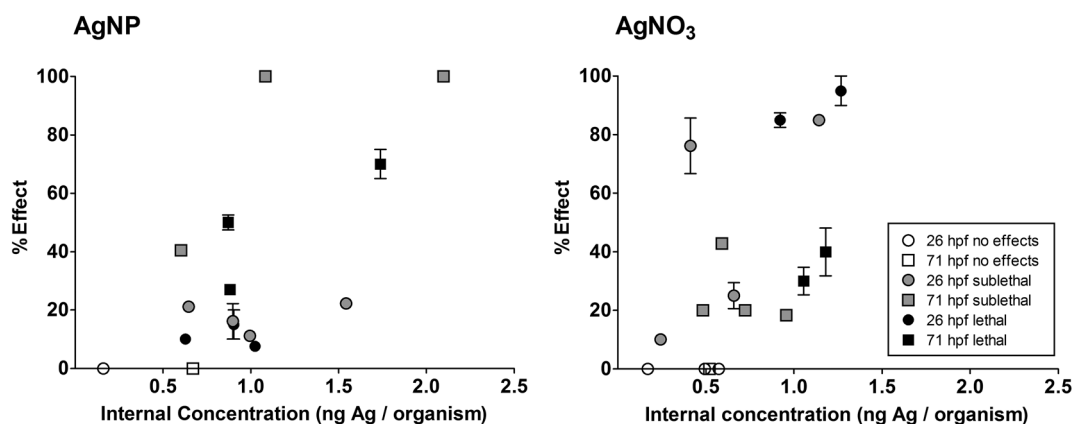


Fig. 5 Correlation between the observed toxicological effects and internal silver concentrations. The measured uptake concentrations and effects for chorion-free developmental stages (26 hpf, 71 hpf) for ZFE showing no effects (empty symbols), sublethal (grey filled symbols), and dead ZFE (black filled symbols) are shown.



attachment and deposition processes and hence no thermodynamic equilibrium as for organic substances is formed.³⁴ Thus, the NP accumulation can be considered as an irreversible step and the deposition of a critical mass of particles can trigger the occurrence of biological effects. Importantly, this effect interferes with the partitioning behaviour of silver ions which simultaneously interact with the ZFE.

Implications for the ZFE as model for NP testing

From our point of view, the ZFE is a suitable biological model for the testing of NPs when certain aspects specific to these materials are considered.

For example, the impact of the ionic fraction released from NP surfaces has to be regarded since ions are actually the chemical component mainly triggering the toxicological effects. However, as described by Cunningham *et al.*¹⁷ all NP test solutions should be regarded as a mixture of AgNPs, aggregates, silver complexes, and dissolved silver ions, which is relevant for both analytical and toxicity studies. Moreover, analytically measured exposure concentrations should be the basis for reliable and comparable dose–response calculations.

The complex influence of the ZFE chorion on the amount of substance taken up needs further attention with regard to accumulation studies. Indeed, the determination of internal concentrations often refers to the whole organism including the chorion. This does not reflect real internal concentrations as the chorion acts as a biological barrier, resulting in concentration overestimation.³⁵ Therefore, we recommend a dechoriation before performing accumulation studies or prior to the analytical measurement. Especially, for the correlation of toxicological effects and uptake amounts, it is favorable to refer to the internal silver concentrations measured for the isolated embryo.

Conclusion

We analysed embryos of different developmental stages and compared the internal concentration and distribution of silver after exposure to AgNPs and AgNO₃ by applying a suite of ICP-MS-based techniques optimised for measuring NPs. Small differences in silver toxicity were observed between the different developmental stages and particulate and ionic silver, respectively by correcting the exposure concentrations for measured concentrations. On the basis of internal silver concentrations, the embryo stage with chorion accumulated substantially more silver compared to the later stages without the chorion, assuming the adsorption of silver to the chorion structures. However, substantial differences in silver distribution were observed when the embryos affected by silver exposure were compared to unaffected ones.

Analytical techniques allowing the differentiation of particle and ionic fractions in one organism would highly contribute to our understanding of especially silver particle toxicity in future studies. Further, the inclusion of more time points would help to gain deeper insight into the toxicological effect

progression. The PVS as a ZFE compartment neglected in this study needs consideration which requires improved sampling procedures.

This study is of general relevance, as the procedure is applicable to other test organisms (*e.g.* daphnids) and NPs. In addition, new insights into the mechanisms and processes on NP–organism interactions were provided which are essential to further improve the risk assessment of such materials.

Acknowledgements

This research was funded by the EU FP7 project NanoValid (Development of reference methods for hazard identification, risk assessment and LCA of engineered nanomaterials; grant no 263147). Additionally, S. B. was kindly supported by the Helmholtz Impulse and Networking Fund through the Helmholtz Interdisciplinary Graduate School for Environmental Research (HIGRADE).

References

- O. J. Osborne, B. D. Johnston, J. Moger, M. Balousha, J. R. Lead, T. Kudoh and C. R. Tyler, *Nanotoxicology*, 2013, 7, 1315–1324.
- C. Völker, T. Gräf, I. Schneider, M. Oetken and J. Oehlmann, *Environ. Sci. Pollut. Res.*, 2014, 21, 10661–10670.
- B. I. Escher and J. L. Hermens, *Environ. Sci. Technol.*, 2004, 38, 455A–462A.
- P. Asharani, Y. Lianwu, Z. Gong and S. Valiyaveetil, *Nanotoxicology*, 2011, 5, 43–54.
- N. R. Brun, M. Lenz, B. Wehrli and K. Fent, *Sci. Total Environ.*, 2014, 476, 657–666.
- D. Chen, D. Zhang, C. Y. Jimmy and K. M. Chan, *Aquat. Toxicol.*, 2011, 105, 344–354.
- S. Scholz, S. Fischer, U. Gündel, E. Küster, T. Luckenbach and D. Voelker, *Environ. Sci. Pollut. Res.*, 2008, 15, 394–404.
- S. El-Amrani, J. Sanz-Landaluze, J. Guinea and C. Camara, *Talanta*, 2013, 104, 67–74.
- A. Kühnert, C. Vogs, R. Altenburger and E. Küster, *Environ. Toxicol. Chem.*, 2013, 32, 1819–1827.
- B. J. Marquis, S. A. Love, K. L. Braun and C. L. Haynes, *Analyst*, 2009, 134, 425–439.
- P. Asharani, Y. L. Wu, Z. Gong and S. Valiyaveetil, *Nanotechnology*, 2008, 19, 1–8.
- K. Fent, C. J. Weisbrod, A. Wirth-Heller and U. Piesles, *Aquat. Toxicol.*, 2010, 100, 218–228.
- S. Lin, Y. Zhao, T. Xia, H. Meng, Z. Ji, R. Liu, S. George, S. Xiong, X. Wang and H. Zhang, *ACS Nano*, 2011, 5, 7284–7295.
- S. Böhme, H.-J. Stärk, D. Kühnel and T. Reemtsma, *Anal. Bioanal. Chem.*, 2015, 407, 5477–5485.
- S. Böhme, H.-J. Stärk, T. Meißner, A. Springer, T. Reemtsma, D. Kühnel and W. Busch, *J. Nanopart. Res.*, 2014, 16, 1–15.
- C. R. Bowman, F. C. Bailey, M. Elrod-Erickson, A. M. Neigh and R. R. Otter, *Environ. Toxicol. Chem.*, 2012, 31, 1793–1800.



- 17 S. Cunningham, M. E. Brennan-Fournet, D. Ledwith, L. Byrnes and L. Joshi, *Environ. Sci. Technol.*, 2013, **47**, 3883–3892.
- 18 OECD, Test No. 236: Fish Embryo Acute Toxicity (FET) Test, www.oecd.org, 2013.
- 19 EU-project NanoValid, *ENP Specification Form Silver Nanoparticles (NNV-003)*, 2014.
- 20 Visual MINTEQ, Version 3.1, 2013, Department of Land and Water Resources Engineering, KTH, Sweden, Available at: <http://vminteq.lwr.kth.se/>.
- 21 K. J. Groh, T. Dalkvist, F. Piccapietra, R. Behra, M. J.-F. Suter and K. Schirmer, *Nanotoxicology*, 2015, **81**–91.
- 22 OECD, *Guidance Document on Aquatic Toxicity Testing of Difficult Substances and Mixtures*, www.oecd.org, 2000.
- 23 D. Kühnel and C. Nickel, *Sci. Total Environ.*, 2014, **472**, 347–353.
- 24 R. van Aerle, A. Lange, A. Moorhouse, K. Paszkiewicz, K. Ball, B. D. Johnston, E. de-Bastos, T. Booth, C. R. Tyler and E. M. Santos, *Environ. Sci. Technol.*, 2013, **47**, 8005–8014.
- 25 O. Bar-Ilan, R. M. Albrecht, V. E. Fako and D. Y. Furgeson, *Small*, 2009, **5**, 1897–1910.
- 26 Y. Yue, R. Behra, L. Sigg, P. F. Freire, S. Pillai and K. Schirmer, *Nanotoxicology*, 2015, **9**, 54–63.
- 27 C. B. Kimmel, W. W. Ballard, S. R. Kimmel, B. Ullmann and T. F. Schilling, *Dev. Dyn.*, 1995, **203**, 253–310.
- 28 M. Auffan, C. W. Matson, J. Rose, M. Arnold, O. Proux, B. Fayard, W. Liu, P. Chaurand, M. R. Wiesner and J.-Y. Bottero, *Nanotoxicology*, 2014, **8**, 167–176.
- 29 S. George, S. Lin, Z. Ji, C. R. Thomas, L. Li, M. Mecklenburg, H. Meng, X. Wang, H. Zhang and T. Xia, *ACS Nano*, 2012, **6**, 3745–3759.
- 30 K. J. Lee, P. D. Nallathamby, L. M. Browning, C. J. Osgood and X.-H. N. Xu, *ACS Nano*, 2007, **1**, 133–143.
- 31 C. M. Powers, T. A. Slotkin, F. J. Seidler, A. R. Badireddy and S. Padilla, *Neurotoxicol. Teratol.*, 2011, **33**, 708–714.
- 32 K. J. Lee, L. M. Browning, P. D. Nallathamby, T. Desai, P. K. Cherukuri and X.-H. N. Xu, *Chem. Res. Toxicol.*, 2012, **25**, 1029–1046.
- 33 X. Zhu, L. Zhu, Z. Duan, R. Qi, Y. Li and Y. Lang, *J. Environ. Sci. Health, Part A: Toxic/Hazard. Subst. Environ. Eng.*, 2008, **43**, 278–284.
- 34 A. Praetorius, N. Tufenkji, K.-U. Goss, M. Scheringer, F. von der Kammer and M. Elimelech, *Environ. Sci.: Nano*, 2014, **1**, 317–323.
- 35 S. Brox, A. P. Ritter, E. Küster and T. Reemtsma, *Aquat. Toxicol.*, 2014, **157**, 134–140.

